ISTS-2017-d-081／ISSFD-2017-081

Flight Control Stability of Multi-Hierarchy Dynamic Inversion for Winged Rocket

By Hiroshi YAMASAKI[1)], Koichi YONEMOTO[1)], Takahiro FUJIKAWA[1)], Kent SHIRAKATA[1)], and Hayato TOBIYAMA[1)]

[1)]*Department of Mechanical and Control Engineering, Kyushu Institute of Technology, Fukuoka, Japan*

(Received June 21st, 2017)

This paper presents stability analysis of a nonlinear control system using hierarchy dynamic inversion (hierarchy DI / Feedback Linearization) combined with block strict-feedback form for a space transportation system. Flight dynamics of space transportation system has wide range aerodynamic characteristics. DI theory enables to cancel the nonlinearity dynamics, and its can be linearized between the input and output maps. Proposed studies of hierarchy dynamic inversion utilized time scale separation. That is think that the response of fast time scale dynamics is be able to neglect, and the controller is designed by consideration of only slow time scale dynamics. However, it is impossible to ignore the response of the fast time scale. Therefore, design of the gain that is able to decide the response speed was the experience of the designer. Here, this controller has the problem that it is difficult to realize the responsiveness desired by the designer while guarantee stability. Authors analyzed the stability by considering the response characteristics of the lower hierarchy using block-strict-feedback form instead of the time scale separation. At this time, a linearized approximation transfer function(LATF) was constructed as assuming that the influence of nonlinear terms is little. However, the influence of nonlinear terms can not be evaluated by LATF. Therefore, the influence of nonlinear terms evaluates using the eigenvalues of the linearized transfer function around momentary state of short period time.

Key Words: Winged Rocket, Nonlinear Dynamics, Stability Analysis, Autonomous Control, Multi-Hierarchy Dynamic Inversion

Nomenclature

V_c	:	velocity of the center of gravity
α,β	:	angle of attack, sideslip angle
Φ,Θ,Ψ	:	zyx-euler roll, pitch, and yaw angles
h,Γ,χ	:	altitude, path, azimuth angles
P,Q,R	:	roll, pitch, yaw angular velocities
I	:	inertia tensor
$I_{xx,yy,zz}$	:	moments of inertia around X, Y and Z axis
I_{xz}	:	product of inertia
M_0	:	Mach number
m	:	vehicle mass
ρ,g	:	air density, gravitational acceleration
$S,b,\bar{c}$	:	wing area, wing span, and mean aerodynamic chord
$\delta_{a,e,r}$	:	aileron, elevator, rudder angle
v_c	:	velocity of the conter of gravity of the perturbation short period time
α_b,β_b	:	angle of attack, sideslip angle of the perturbation short period time
ϕ,θ	:	zyx-euler roll, pitch angles of the perturbation short period time
p,q,r	:	roll, pitch, yaw angular velocities of the perturbation short period time
δ_{a_b,e_b,r_b}	:	aileron, elevator, rudder angle of the perturbation short period time
$\delta_{eL,eR}$	:	elevon left, and elevon right angle
K_i	:	control gains ($i = \alpha,\beta,\phi,\dot{\alpha},\dot{\beta},\dot{\phi}$)
$\omega_{\alpha,\beta,\phi}$	:	controlled natural frequencies
ζ_i	:	controlled damping coefficients
$\omega_{\delta_{a,e,r}}$	:	natural frequencies of actuators
$\zeta_{\delta_{a,e,r}}$	:	damping coefficients of actuators
r	:	relative degree
n	:	dimension of vectors
m	:	hierarchical number
k	:	control input number
$\mathbf{x}_i$	:	state vectors
$\mathbf{y}_i$	:	controlled variables of i-th hierarchical structure
$\mathbf{y}_{i_{\mathrm{ref}}}$	:	reference of controlled valuables of i-th hierarchical structure
u	:	manipulated variables
v_i	:	pseudo inputs of i-th hierarchical structure
F_i,G_i	:	affine system of i-th hierarchical structure
$L_f{}^r$	:	r-degrees Lie derivative of f-function
J_i	:	jacobian matrix of i-th hierarchical structure
$J_{i,jk}$	:	j-k component of jacobian matrix of i-th hierarchical structure
E	:	identity matrix
σ_i	:	substituted variables

Subscripts

$(\ )_{\mathrm{lon,lat}}$	:	functions of longitudinal equation, lateral directional equation

$( )_0$: equilibrium point of short period time

$( )_{ref}$: reference of each controlled valuables

1. Introduction

In 2004, SpaceShipOne made by Space Composites was succeeded the flight to reach an altitude of 100 km as the first manned space flight by a private company. In recent years, Falcon 9 that is low cost, and reusable transportation system made by SpaceX is attracting. In this way, development of reusable space transportation system facility for commercial has been actively all around the world to facilitate space travel at low cost. Such a system has strong nonlinear, because the flight profile has a wide range of dynamic characteristics. Under such circumstances, realizing autonomous control by a computer has a huge impact in the future space transportation system. Therefore, there is an increasing necessity to develop autonomous nonlinear control laws for realization of space transportation system.

The authors focus on developing dynamic inversion (DI) theory for realization of nonlinear control law. DI theory is controller technique that cancelled nonlinear dynamics of the system, and give desirable dynamics by algebraic transformation[1-3]. However, In DI theory there are difficulties to construct the control law if the system has high relative degree between the input and output maps. Menon et al., research on flight control based on DI theory combined with time-scale separation has been actively conducted[4-5]. Many researchers utilized these researched reports[6-9], and summarized them in a survey[10]. Time-scale separation is a concept derived from singular perturbation theory[11], it enables to construct the hierarchical dynamics when the vehicle dynamic characteristics for each subsystem are explicit difference. This concept has a potential for all of the system. This concept has a potential exist in all of the system, if the system has the explicit different time constants. And also, If control law is able to be given the time constants with the different systems properly, dynamics variables enable time-scale separation construct the hierarchical to reduce the complexity of a dynamical system and can greatly simplify the control law and analysis problem. Outer loop of time-scale separation has relatively small time constant called as “slow-scale”, Inner loop has conversely high time constant called as "fast-scale". According to Baba et al., the ratio between the time constant of fast scale and the one of slow scale stated necessary around four times[7].

Kawaguchi et al, developed control system of the experimental aircraft called “D-SEND” for low sonic boom design concept[12-14]. D-SEND#2 is adopted the DI control law using time-scale separation, it was successfully recovered. There is a report that the number of control gain has been drastically reduced compared to the previous control laws, its effectiveness is also shown[15].

However, in the control law of slow-scale subsystem design, time-scale separation assumes that dynamic variable of fast-scale reached already an equilibrium state. Therefore, dynamics interference between the subsystems is disregarded, and there are also some research reports stating that it is difficult to guarantee the stability of a closed-loop system. In addition, in case of the design of control gains of time-scale separation needs an empirical element, and if the time constants ratio between fast scale and slow scale is not properly, the control performance deteriorates than expected by designed.

Abe, Iwamoto, Shimada constructed the adaptive control law using backstepping methodology that guarantees lyapunov stability for these problem[16,17]. Generally, constructing the control law using backstepping methodology, derivative of intermediate manipulated variables of each hierarchy is needed. This problem makes the analysis even more difficult, and the control law becomes complicated. Their research is extremely interesting that it is possible to estimate the derivative of intermediate manipulated variable as unknown parameters, thereby preventing further complication of the control system. Characteristic of the adaptive control using backstepping methodology has robustness to disturbance, and it is possible to stabilize and guarantee the nonlinear closed-loop system. For the actual demonstration, they carried out numerical simulation for ALFLEX (Automatic Landing Flight Experimental) vehicle as a model, indicating that the robustness against disturbance in the lateral direction is improved. If the design of control gains is determined appropriately, it enables to guarantee the lyapunov stability by adaptive control law using backstepping methodology. However, the methodology to determine the control gains is needed to be studied.

Authors construct transfer functions in each hierarchy from the block-strict feedback forms of the backstepping methodology and evaluate the control performance. This research has two purposes. One is to simplify the design of the control law of the DI theory and determine the relationship between the vehicle dynamic characteristics of the closed loop and control gain. The other is effectiveness of gain design methodology is presented from the stability analysis of eigenvalue.

This analysis quantitatively shows the dynamic characteristics of lower hierarchy subsystem affecting the higher hierarchy subsystem. In this analysis, it is not enabled to cancel the nonlinear dynamic characteristics of higher hierarchy completely, because of being affected by the dynamic characteristics of the lower hierarchy. Conversely, if the response speed of the lower subsystem is high enough than the higher subsystem, the effect of the nonlinear dynamic characteristic becomes small, and the effect can expect ignored. This concept is close to the concept of forced singular perturbation theory. Linear approximation dynamic characteristics constructed by this concept enable to evaluate as a linear dynamic characteristic that is not affected by the nonlinear dynamic characteristics of the vehicle. In addition, it constructs short-period time linearization to not ignore nonlinear dynamic characteristics in order to evaluate strictly. Authors compare the eigenvalue using each nonlinear dynamic characteristics, and evaluates the difference of each value. Furthermore, analysis state points utilize each time series from numerical simulations.

Vehicle model adopts WIRES (WInged REusable Sounding rocket) developed by authors. WIRES is the experimental winged rocket for space transportation system under development by the space club of Kyushu Institute of Technology since 2005(Fig. 1). The shape of WIRES is based on HIMES (Highly Maneuverable Experimental Space Vehicle) developed by Japan Aerospace Exploration Agency (JAXA).

From 2008 to 2014, Kyutech developed a small scaled winged rocket called WIRES#011 for ascent phase attitude control, and WIRES#012 for the safety recovery system using two-stages parachute and airbag system[16]. Since 2012, is developing WIRES#014 in order to verify the preliminary technologies of on-board autonomous Navigation Guidance, and Control System. WIRES#014 was developed three times. The third WIRES#014-3 was launched, and recovered successfully in November 2015[17-19]. Since 2014, Kyutech has started to design WIRES#013, and WIRES#015 in order to demonstrate of WIRES-X[19]. In this paper, stability analysis of return phase evaluates using WIRES#015 size as a model. Fig. 2 shows the specification of WIRES#015.

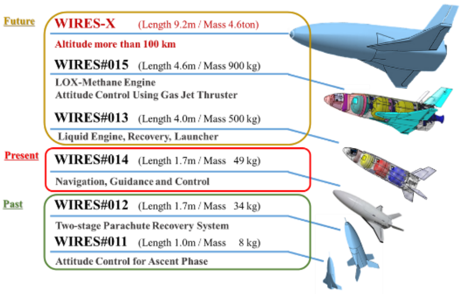

Fig. 1 Development of Winged Rocket "WRIES".

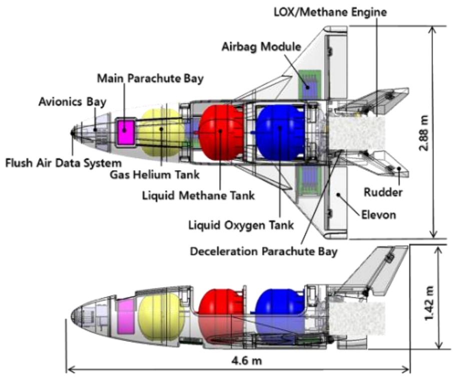

Fig. 2. Subscale winged rocket WIRES#015.

Table 1. Specification of WIRES#015.

Vehicle dry mass	[kg]	672
Total length	[m]	4
Wing area	[m^2]	2.68
Wing span	[m]	2.88
Mean aerodynamic chord	[m]	1.08
Moments of inertia around X axis	[kg m^2]	109
Moments of inertia around Y axis	[kg m^2]	3247
Moments of inertia around Z axis	[kg m^2]	3247
Center of gravity	[%]	66

2. Dynamic inversion

Dynamic inversion is a well-established branch of study in control theory that performs a linearization of the input and output variables by the *n* number of derivatives with respect to the observables in the DI theory. Therefore, it is possible to pseudo-linearize nonlinear state equations.

2.1. Dynamic inversion theory of MISO system

Dynamic Inversion Theory is the linearization methodology between input output maps for nonlinear dynamics. Albertio Ishidori proposed the control law using nonlinearity of affine system[1]. In this section, it is introduce the method the control system using the dynamic inversion theory of Multi Input Multi Output(MIMO) system. The target system is affine system, and it is expressed as follows.

$$\begin{aligned} \dot{\mathbf{x}} &= f(\mathbf{x}) + \sum_{i=1}^{k} g_i(\mathbf{x}) u_i \\ \mathbf{y} &= h(\mathbf{x}) \end{aligned} \tag{1}$$

These mappings may be represented in the form of n-dimensional vectors of real-valued functions.

$$f(\mathbf{x}) = \begin{pmatrix} f_1(\mathbf{x}) \\ f_2(\mathbf{x}) \\ \vdots \\ f_n(\mathbf{x}) \end{pmatrix},\ g(\mathbf{x}) = \begin{pmatrix} g_1(\mathbf{x}) \\ g_2(\mathbf{x}) \\ \vdots \\ g_n(\mathbf{x}) \end{pmatrix},\ h(\mathbf{x}) = \begin{pmatrix} h_1(\mathbf{x}) \\ h_2(\mathbf{x}) \\ \vdots \\ h_k(\mathbf{x}) \end{pmatrix}$$

Here, L_f is the Lie derivative and expressed by the following the Eq. (2). And, $L^{i+1}{}_f h$

$$\begin{aligned} L_f h &= \frac{dh}{d\mathbf{x}} f(\mathbf{x}) = \sum_{i=1}^{n} \frac{\partial h}{\partial x_i} f_i(\mathbf{x}) \\ L^{i+1}{}_f h &= L_f\left(L^i{}_f h\right),\ i = 1,2,\ldots,r-1 \end{aligned} \tag{2}$$

The relative degree means the derivative times until the controlled valuables appears, and the sufficient conditions are expressed as follows.

$$\begin{cases} L_g\left(L_f^j h\right) = \sum_{i}^{n} \dfrac{\partial L_f h_k}{\partial x_i} g_i = 0 & j = 0,1,2,\ldots,r_k - 2 \\ L_g\left(L_f^j h\right) = \sum_{i}^{n} \dfrac{\partial L_f h_k}{\partial x_i} g_i \neq 0 & j = r - 1 \end{cases} \tag{3}$$

Such a system has a vector relative degree $\{r_1,\ldots,r_k\}$. When this time lie derivative matrix of each controlled valuables is expressed by the following Eq. (4).

$$\mathbf{z} = B + Au \tag{4}$$

$$\mathbf{z} = \begin{pmatrix} y_1^{(r_1)} \\ y_2^{(r_2)} \\ \vdots \\ y_k^{(r_k)} \end{pmatrix},\quad B = \begin{bmatrix} L_f^{r_1} h_1(\mathbf{x}) \\ L_f^{r_2} h_2(\mathbf{x}) \\ \vdots \\ L_f^{r_k} h_k(\mathbf{x}) \end{bmatrix}$$

$$A = \begin{bmatrix} L_{g_1} L_f^{r_1-1} h_1(\mathbf{x}) & \cdots & L_{g_k} L_f^{r_1-1} h_1(\mathbf{x}) \\ L_{g_1} L_f^{r_2-1} h_2(\mathbf{x}) & \cdots & L_{g_k} L_f^{r_2-1} h_2(\mathbf{x}) \\ \vdots & \ddots & \vdots \\ L_{g_1} L_f^{r_k-1} h_k(\mathbf{x}) & \cdots & L_{g_k} L_f^{r_k-1} h_k(\mathbf{x}) \end{bmatrix}$$

Therefore, inverse dynamics of MIMO affine system from manipulated variables to controlled variables is expressed by the following Eq. (5) that is transformed Eq. (4).

$$u = A^{-1}(\mathbf{z} - B) \tag{5}$$

Generally, z is a vector of derivatives of y. Then, rearranging the vector of derivative of y to pseudo input ν, dynamic inversion controller is completed. Here, pseudo input ν is the design parameter that is able to decide arbitrarily.

$$u = \frac{1}{L_g L^{n-1}{}_f h}\left(\nu - L^n{}_f h\right) \tag{6}$$

The designed property and the stability control law stabilize the controlled variables.

3. Vehicle dynamics and control system

Vehicle dynamics is able to separate the rocket dynamics model (first hierarchy) and actuator dynamics model(second hierarchy). Then, in this case, vehicle dynamics has two hierarchical structures, each dynamics are expressed as follows.

$$\begin{bmatrix}\dot{\mathbf{x}}_1\\ \dot{\mathbf{x}}_2\end{bmatrix} = \begin{bmatrix}F_1(\mathbf{x}_1)\\ F_2(\mathbf{x}_2)\end{bmatrix} + \begin{bmatrix}G_1(\mathbf{x}_1)\mathbf{y}_2\\ G_2(\mathbf{x}_2)u\end{bmatrix}$$

$$\mathbf{y}_1 = h_1(\mathbf{x}_1) = \begin{bmatrix}\alpha\\ \beta\\ \Phi\end{bmatrix}, \mathbf{y}_2 = h_2(\mathbf{x}_2) = \begin{bmatrix}\delta_a\\ \delta_e\\ \delta_r\end{bmatrix} \tag{7}$$

$$\mathbf{x}_1 = [V_c \quad \alpha \quad \beta \quad P \quad Q \quad R \quad \Phi \quad \Theta]^T$$

$$\mathbf{x}_2 = [\delta_a \quad \dot{\delta}_a \quad \delta_e \quad \dot{\delta}_e \quad \delta_r \quad \dot{\delta}_r]^T$$

$$F_1(\mathbf{x}_1) = \begin{bmatrix} f_{1,1}(\mathbf{x}_1)\\ f_{1,2}(\mathbf{x}_1)\\ f_{1,3}(\mathbf{x}_1)\\ f_{1,4}(\mathbf{x}_1)\\ f_{1,5}(\mathbf{x}_1)\\ f_{1,6}(\mathbf{x}_1)\\ f_{1,7}(\mathbf{x}_1)\\ f_{1,8}(\mathbf{x}_1)\end{bmatrix}, F_2(\mathbf{x}_2) = \begin{bmatrix} f_{2,1}(\mathbf{x}_{1,2})\\ f_{2,2}(\mathbf{x}_{1,2})\\ f_{2,3}(\mathbf{x}_{1,2})\\ f_{2,4}(\mathbf{x}_{1,2})\\ f_{2,5}(\mathbf{x}_{1,2})\\ f_{2,6}(\mathbf{x}_{1,2})\end{bmatrix}$$

$$G_1(\mathbf{x}_1) = \begin{bmatrix} 0 & 0 & 0\\ 0 & 0 & 0\\ 0 & 0 & 0\\ g_{1,41}(\mathbf{x}_1) & 0 & g_{1,43}(\mathbf{x}_1)\\ 0 & g_{1,52}(\mathbf{x}_1) & 0\\ g_{1,61}(\mathbf{x}_1) & 0 & g_{1,63}(\mathbf{x}_1)\\ 0 & 0 & 0\\ 0 & 0 & 0\end{bmatrix}$$

$$G_2(\mathbf{x}_2) = \begin{bmatrix} 0\\ g_{2,2}(\mathbf{x}_{1,2})\\ 0\\ g_{4,2}(\mathbf{x}_{1,2})\\ 0\\ g_{6,2}(\mathbf{x}_{1,2})\end{bmatrix}$$

3.1. Vehicle dynamics

Vehicle dynamics has nonlinear 8-vectors (velocity, angle of attack, sideslip angle, angular velocities of each axis, roll angle, and pitch angle) of first hierarchy, and 6-vectors(there actuators of each 2nd order delay) of second hierarchy(Eqs.(8-(11). Regarding to aerodynamics, assuming that the differential coefficient of the control surfaces is proportional, it can be treated as an affine system(Eq. (12)).

$$\begin{bmatrix} f_{1,1}(\mathbf{x}_1)\\ f_{1,2}(\mathbf{x}_1)\\ f_{1,3}(\mathbf{x}_1)\\ f_{1,4}(\mathbf{x}_1)\\ f_{1,5}(\mathbf{x}_1)\\ f_{1,6}(\mathbf{x}_1)\\ f_{1,7}(\mathbf{x}_1)\\ f_{1,8}(\mathbf{x}_1)\end{bmatrix} = \begin{Bmatrix} V_g + \dfrac{\rho V_c{}^2 S}{2m}\left(C_Y(\alpha,\beta,M_0,P,R)\sin\beta - C_D(\alpha,M_0)\cos\beta\right)\\ Q - \tan\beta(P\cos\alpha + R\sin\alpha) + \alpha_g - \dfrac{\rho V_c S}{2m\cos\beta}C_L(\alpha,M_0)\\ \cos\alpha(P-R) + \beta_g + \dfrac{\rho V_c S}{2m}\left(C_Y(\alpha,\beta,M_0,P,R)\cos\beta + C_D(\alpha,M_0)\sin\beta\right)\\ I^{-1}\left\{\dfrac{1}{2}\rho V_c{}^2 S\begin{bmatrix} bC'_l(\alpha,\beta,M_0,P,R)\\ \bar{c}C'_M(\alpha,\dot{\alpha},M_0,Q)\\ bC'_n(\alpha,\beta,M_0,P,R)\end{bmatrix} - \begin{bmatrix}P\\ Q\\ R\end{bmatrix}\times\left(I\begin{bmatrix}P\\ Q\\ R\end{bmatrix}\right)\right\}\\ P + R\cos\Phi\tan\Theta + Q\sin\Phi\tan\Theta\\ Q\cos\Phi - R\sin\Phi \end{Bmatrix} \tag{8}$$

$$\begin{bmatrix} f_{2,1}(\mathbf{x}_2)\\ f_{2,2}(\mathbf{x}_2)\\ f_{2,3}(\mathbf{x}_2)\\ f_{2,4}(\mathbf{x}_2)\\ f_{2,5}(\mathbf{x}_2)\\ f_{2,6}(\mathbf{x}_2)\end{bmatrix} = \begin{bmatrix} 0 & 1 & 0 & 0 & 0 & 0\\ -\omega_{\delta_a}{}^2 & -2\zeta_{\delta_a}\omega_{\delta_a} & 0 & 0 & 0 & 0\\ 0 & 0 & 0 & 1 & 0 & 0\\ 0 & 0 & -\omega_{\delta_e}{}^2 & -2\zeta_{\delta_e}\omega_{\delta_e} & 0 & 0\\ 0 & 0 & 0 & 0 & 0 & 1\\ 0 & 0 & 0 & 0 & -\omega_{\delta_r}{}^2 & -2\zeta_{\delta_r}\omega_{\delta_r}\end{bmatrix}\begin{bmatrix}\delta_a\\ \dot{\delta}_a\\ \delta_e\\ \dot{\delta}_e\\ \delta_r\\ \dot{\delta}_r\end{bmatrix} \tag{9}$$

$$\begin{bmatrix} g_{1,41}(\mathbf{x}_1) & 0 & g_{1,43}(\mathbf{x}_1)\\ 0 & g_{1,52}(\mathbf{x}_1) & 0\\ g_{1,61}(\mathbf{x}_1) & 0 & g_{1,63}(\mathbf{x}_1)\end{bmatrix} = \frac{1}{2}\rho V_c{}^2 S I^{-1}\begin{bmatrix} bC_{l_{\delta_a}} & 0 & bC_{l_{\delta_r}}\\ 0 & \bar{c}C_{m_{\delta_e}} & 0\\ bC_{n_{\delta_a}} & 0 & bC_{n_{\delta_r}}\end{bmatrix} \tag{10}$$

$$\begin{pmatrix} V_g \\ \alpha_g \\ \beta_g \end{pmatrix} = \begin{pmatrix} -g(\cos\beta\cos\alpha\sin\Theta - \sin\beta\sin\Phi\cos\Theta - \cos\beta\sin\alpha\cos\Phi\cos\Theta) \\ \dfrac{g}{V_c\cos\beta}(\sin\alpha\sin\Theta + \cos\alpha\cos\Phi\cos\Theta) \\ \dfrac{g}{V_c}(\cos\beta\cos\Theta\sin\Phi + \sin\beta\cos\alpha\sin\Theta - \sin\beta\sin\alpha\cos\Theta\cos\Phi) \end{pmatrix} \tag{11}$$

$$\begin{aligned} C_l(\alpha, M_0, \beta, P, R, \delta_a, \delta_r) &\cong C_l'(\alpha, M_0, \beta, P, R) + C_{l_{\delta_a}}(\alpha, M_0)\delta_a + C_{l_{\delta_r}}(\alpha, M_0)\delta_r \\ C_M(\alpha, \dot{\alpha}, M_0, Q, \delta_e) &\cong C_M'(\alpha, \dot{\alpha}, M_0, Q) + C_{m_{\delta_e}}(\alpha, M_0)\delta_e \\ C_N(\alpha, M_0, \beta, P, R, \delta_a, \delta_r) &\cong C_N'(\alpha, M_0, \beta, P, R) + C_{n_{\delta_a}}(\alpha, M_0)\delta_a + C_{n_{\delta_r}}(\alpha, M_0)\delta_r \end{aligned} \tag{12}$$

3.2. Design control law

Design control method is follow Ref. 20). This method generates desired value of lower hierarchy for each hierarchy. Assuming that the design of the actuator is already, generally, it is able to be assumed that the response characteristic of the actuator has a second-order lag. Therefore, controller of the vehicle necessary is only required the dynamic inversion controller obtained from angle of attack, side slip angle, and bank angle to the control surfaces. Here, it is assumed that the calculation from the target position to the target angle of attack, side slip angle, bank angle are generated by the guidance law, and is excluded from the analysis of this study.

In this section, it will treated as the design method of control law from the target angle of attack, side slip angle, bank angle to control surfaces using hierarchy dynamic inversion.

$$\mathbf{y}_1 = h_1(\mathbf{x}_1) = \begin{bmatrix} \alpha \\ \beta \\ \Phi \end{bmatrix} \tag{13}$$

$$\mathbf{y}_1^{(1)} = L_{F_1}h(\mathbf{x}_1) + L_{G_1}h(\mathbf{x}_1) \tag{14}$$

$$\begin{bmatrix} \dot{\alpha} \\ \dot{\beta} \\ \dot{\Phi} \end{bmatrix} = \begin{bmatrix} f_{1,2}(\mathbf{x}_1) \\ f_{1,3}(\mathbf{x}_1) \\ f_{1,7}(\mathbf{x}_1) \end{bmatrix}, \ (L_{G_1}h(\mathbf{x}) = 0)$$

It does the time derivative once again.

$$\mathbf{y}_1^{(2)} = L_{F_1}^2 h(\mathbf{x}_1) + L_{F_1}L_{G_1}h(\mathbf{x}_1) \tag{15}$$

Eq. (15) can be expressed concretely as follows.

$$\mathbf{y}_1^{(2)} = h_1^T(\mathbf{x}_1)J_1(\mathbf{x}_1)F_1(\mathbf{x}_1) + h_1^T(\mathbf{x}_1)J_1(\mathbf{x}_1)G_1(\mathbf{x}_1)\mathbf{y}_2 \tag{16}$$

where $J(\mathbf{x})$ is the Jacobian of the model dynamics.

$$\ddot{\mathbf{x}}_1 = J_1(\mathbf{x}_1)\dot{\mathbf{x}}_1$$

Therefore, inverse dynamics of Eq. (16) becomes as follows.

$$\mathbf{y}_2 = \frac{1}{h_1^T(\mathbf{x}_1)J_1(\mathbf{x}_1)G_1(\mathbf{x}_1)}\left\{\mathbf{y}_1^{(2)} - h_1^T(\mathbf{x}_1)J_1(\mathbf{x}_1)F_1(\mathbf{x}_1)\right\} \tag{17}$$

Here, control command is constructed by replacing $\mathbf{y}_1^{(2)}$ to pseudo input ν_1. In this case, relative degree of first hierarchy is 2-degrees. When the design of the pseudo input

$$\nu_1 = \begin{bmatrix} K_\alpha(\alpha_{\text{ref}} - \alpha) - K_{\dot{\alpha}}\dot{\alpha} \\ K_\beta(\beta_{\text{ref}} - \beta) - K_{\dot{\beta}}\dot{\beta} \\ K_\phi(\Phi_{\text{ref}} - \Phi) - K_{\dot{\phi}}\dot{\Phi} \end{bmatrix} = K_P(\mathbf{y}_{1_{\text{ref}}} - \mathbf{y}_1) + K_D\dot{\mathbf{y}}_1 \tag{18}$$

$$K_P = \text{diag}(K_\alpha \quad K_\beta \quad K_\phi), K_D = \text{diag}(K_{\dot{\alpha}} \quad K_{\dot{\beta}} \quad K_{\dot{\phi}})$$

$$\mathbf{y}_{1_{\text{ref}}} = [\alpha_{\text{ref}} \quad \beta_{\text{ref}} \quad \Phi_{\text{ref}}]^T, \mathbf{y}_1 = [\dot{\alpha} \quad \dot{\beta} \quad \dot{\Phi}]^T$$

$$\mathbf{y}_2 = \frac{1}{h_1^T(\mathbf{x}_1)J_1(\mathbf{x}_1)G_1(\mathbf{x}_1)}\left\{\nu_1 - h_1^T(\mathbf{x}_1)J_1(\mathbf{x}_1)F_1(\mathbf{x}_1)\right\} \tag{19}$$

Ideal response is becomes the next equation.

$$\begin{aligned} P_\alpha(s) &= \frac{K_\alpha}{s^2 + K_{\dot{\alpha}}s + K_\alpha} \\ P_\beta(s) &= \frac{K_\beta}{s^2 + K_{\dot{\beta}}s + K_\beta} \\ P_\phi(s) &= \frac{K_\phi}{s^2 + K_\phi s + K_\phi} \end{aligned} \tag{20}$$

These response characteristics of transfer function [eq.(20)] are equal to the response characteristics that designed by time scale separation. The control designer can determine these gains, and it is possible to select damping factors and each natural frequencies.

$$\begin{aligned} K_\alpha &= \omega_\alpha{}^2 \ , \ K_{\dot{\alpha}} = 2\zeta_\alpha\omega_\alpha \\ K_\beta &= \omega_\beta{}^2 \ , \ K_{\dot{\beta}} = 2\zeta_\beta\omega_\beta \\ K_\phi &= \omega_\phi{}^2 \ , \ K_{\dot{\phi}} = 2\zeta_\phi\omega_\phi \end{aligned} \tag{21}$$

However, actual response includes delay of second hierarchy characteristics. It is assumed that the delay characteristics of each actuators are second order delay.

$$\begin{aligned} P_{\delta_a}(s) &= \frac{\omega_{\delta_a}{}^2}{s^2 + 2\zeta_{\delta_a}\omega_{\delta_a}s + \omega_{\delta_a}{}^2} \\ P_{\delta_e}(s) &= \frac{\omega_{\delta_e}{}^2}{s^2 + 2\zeta_{\delta_e}\omega_{\delta_e}s + \omega_{\delta_e}{}^2} \\ P_{\delta_r}(s) &= \frac{\omega_{\delta_r}{}^2}{s^2 + 2\zeta_{\delta_r}\omega_{\delta_r}s + \omega_{\delta_r}{}^2} \end{aligned} \tag{22}$$

Next, assuming Eq. (19) which is the control law at the first hierarchy of Eq. (7), and considering Eq. (22) which is the delay characteristic of the second hierarchy, it becomes the following equation.

$$
\mathbf{y}_1^{(2)} = L_{F_1}^2 h(\mathbf{x}_1) + L_{G_1} L_{F_1} h(\mathbf{x}_1) \begin{bmatrix} P_{\delta_a} & 0 & 0 \\ 0 & P_{\delta_e} & 0 \\ 0 & 0 & P_{\delta_r} \end{bmatrix} \left\{ L_{G_1} L_{F_1} h(\mathbf{x}_1) \right\}^{-1} \left\{ \nu_1 - L_{F_1}^2 h(\mathbf{x}_1) \right\} \qquad (23)
$$

Here, actuators has same response characteristics as follows.

$$
P_\delta(s) = P_{\delta_a}(s) = P_{\delta_e}(s) = P_{\delta_r}(s) \qquad (24)
$$

The Eq. (23) can be transform as follows.

$$
\mathbf{y}_2^{(2)} = L_{F_1}^2 h(\mathbf{x}_1)(E - P_\delta) + P_\delta \nu_1 \qquad (25)
$$

When it is ignore the nonlinear terms following the hierarchy dynamic inversion, Eq. (25) can approximate to the next equation.

$$
\mathbf{y}_2^{(2)} \cong P_\delta \nu_1 \qquad (26)
$$

And then, transfer function is expressed as follows.

$$
\begin{aligned}
P_\alpha(s) &= \frac{\omega_\alpha{}^2 P_\delta}{s^2 + 2\zeta_\alpha \omega_\alpha s P_\delta + \omega_\alpha{}^2 P_\delta} \\
P_\beta(s) &= \frac{\omega_\beta{}^2 P_\delta}{s^2 + 2\zeta_\beta \omega_\beta s P_\delta + \omega_\beta{}^2 P_\delta} \qquad (27) \\
P_\phi(s) &= \frac{\omega_\phi{}^2 P_\delta}{s^2 + 2\zeta_\phi \omega_\phi s P_\delta + \omega_\phi{}^2 P_\delta}
\end{aligned}
$$

In this paper, it is call Linearized Approximation Transfer Function(LATF).

4. Short period time model

Previous chapter, the LATF is not dependent on of the vehicle dynamics is derived for designing the control law. However, LATF is ignore the nonlinear terms of Eq. (25). Therefore, LATF does not express a strict response of the vehicle dynamics.

In generally linear analysis, a trimmed states is generated at each evaluation point. However, hierarchy DI method is necessary not only to linearize the motion equation but also to calculate variables in order to generate control command. Therefore, in this analysis, the stability around the current status is evaluated, and it is judged whether or not an unstable solution exists in eigenvalue analysis. Then, it is analyzed the eigenvalue of the each short period time model, and compared the LATF.

4.1. Longitudinal model

Longitudinal stability can be evaluate motion of longitudinal model of the short period time. In this time, For the dynamics of the aircraft expressed by Eq. (25), linearized with the following .

$$
\begin{aligned}
\mathbf{x}_{1_{\text{lon}}}(t) &= \mathbf{x}_{1_{\text{lon0}}} + x_{1_{\text{lon}}}(t) \\
\mathbf{x}_{2_{\text{lon}}}(t) &= \mathbf{x}_{2_{\text{lon0}}} + x_{2_{\text{lon}}}(t) \qquad (28) \\
\delta_{e_{\text{ref}}}(t) &= \delta_{e_{0\text{ref}}} + \delta_{e_{b\text{ref}}}(t)
\end{aligned}
$$

$$
\begin{cases}
\mathbf{x}_{1_{\text{lon}}}(t) = [V_c(t) \quad \alpha(t) \quad Q(t) \quad \Theta(t)]^T \\
\mathbf{x}_{1_{\text{lon0}}} = [V_{c_0} \quad \alpha_0 \quad Q_0 \quad \theta_0]^T \\
x_{1_{\text{lon}}}(t) = [v_c(t) \quad \alpha_b(t) \quad q(t) \quad \theta(t)]^T
\end{cases}
$$

$$
\begin{cases}
\mathbf{x}_{2_{\text{lon}}}(t) = [\delta_e(t) \quad \dot{\delta}_e(t)]^T \\
\mathbf{x}_{2_{\text{lon0}}} = [\delta_{e_0} \quad 0]^T \\
x_2(t) = [\delta_{e_b}(t) \quad \dot{\delta}_{e_b}(t)]^T
\end{cases}
$$

Here, It assumed that lateral states is equipment states.

$$
\beta = \beta_0, P = P_0, R = R_0, \Phi = \Phi_0 \qquad (29)
$$

When this time, linear system expressed are

$$
\begin{aligned}
\dot{\mathbf{x}}_{1_{\text{lon}}} &= A_{\text{lon}} \mathbf{x}_{1_{\text{lon}}} + B_{\text{lon}} \mathbf{y}_{1_{\text{lon,com}}} \qquad (30) \\
\mathbf{y}_{1_{\text{lon}}} &= C_{\text{lon}} \mathbf{x}_{1_{\text{lon}}}
\end{aligned}
$$

$$
P_{1_{\text{lon}}}(s) = C_{\text{lon}} (sE - A_{\text{lon}})^{-1} B_{\text{lon}} \qquad (31)
$$

Where,

$$
A_{\text{lon}} = \begin{bmatrix}
J_{1,11} & J_{1,12} & J_{1,15} & J_{18} \\
J_{1,21} & J_{1,22} & J_{1,25} & J_{28} \\
J_{1,51} - (J_{1,21}' + 2\xi_\alpha \omega_\alpha J_{1,21}) P_{\delta_e} & J_{1,52} - (J_{1,22}' + 2\xi_\alpha \omega_\alpha J_{1,22} + \omega_\alpha{}^2) P_{\delta_e} & J_{1,55} - (J_{1,23}' + 2\xi_\alpha \omega_\alpha J_{25}) P_{\delta_e} & J_{1,58} - (J_{24}' + 2\xi_\alpha \omega_\alpha J_{28}) P_{\delta_e} \\
J_{81} & J_{82} & J_{85} & J_{88}
\end{bmatrix}
$$

$$
B_{\text{lon}} = \begin{bmatrix} 0 \\ 0 \\ \omega_\alpha{}^2 P_{\delta_e} \\ 0 \end{bmatrix}, \quad C_{\text{lon}} = \begin{bmatrix} 0 \\ 1 \\ 0 \\ 0 \end{bmatrix}^T
$$

$$
\begin{aligned}
\sigma_{1_{\text{lon}}} &= \frac{\partial}{\partial V_c} (J_{1,21} f_{1,1} + J_{1,22} f_{1,2} + J_{1,25} f_{1,5} + J_{1,28} f_{1,8}) \\
\sigma_{2_{\text{lon}}} &= \frac{\partial}{\partial \alpha} (J_{1,21} f_{1,1} + J_{1,22} f_{1,2} + J_{1,25} f_{1,5} + J_{1,28} f_{1,8}) \\
\sigma_{3_{\text{lon}}} &= \frac{\partial}{\partial Q} (J_{1,21} f_{1,1} + J_{1,22} f_{1,2} + J_{1,25} f_{1,5} + J_{1,28} f_{1,8}) \\
\sigma_{4_{\text{lon}}} &= \frac{\partial}{\partial \Theta} (J_{1,21} f_{1,1} + J_{1,22} f_{1,2} + J_{1,25} f_{1,5} + J_{1,28} f_{1,8})
\end{aligned}
$$

4.2. Lateral directional model

Lateral directional stability can be evaluate motion of lateral directional model of the short period time. In this time, For the dynamics of the aircraft expressed by Eq. (32), linearized with the following .

$$
\begin{aligned}
\mathbf{x}_{1_{\text{lat}}}(t) &= \mathbf{x}_{1_{\text{lat0}}}(t) + x_{1_{\text{lat}}}(t) \\
\mathbf{x}_{2_{\text{lat}}}(t) &= \mathbf{x}_{2_{\text{lat0}}}(t) + x_{2_{\text{lat}}}(t) \\
\delta_{a_{\text{ref}}}(t) &= \delta_{a_{0\text{ref}}}(t) + \delta_{a_{b\text{ref}}}(t) \qquad (32) \\
\delta_{r_{\text{ref}}}(t) &= \delta_{r_{0\text{ref}}}(t) + \delta_{r_{b\text{ref}}}(t)
\end{aligned}
$$

$$
\begin{cases}
\mathbf{x}_{1_{\text{lat}}}(t) = [\beta(t) \quad P(t) \quad R(t) \quad \Phi(t)]^T \\
\mathbf{x}_{1_{\text{lat0}}} = [\beta_0 \quad P_0 \quad R_0 \quad \Phi_0]^T \\
x_{1_{\text{lat}}}(t) = [\beta_b(t) \quad p(t) \quad r(t) \quad \phi(t)]^T
\end{cases}
$$

$$
\begin{cases}
\mathbf{x}_{2_{\text{lat}}}(t) = [\delta_a(t) \quad \dot{\delta}_a(t) \quad \delta_r(t) \quad \dot{\delta}_r(t)]^T \\
\mathbf{x}_{2_{\text{lat0}}} = [\delta_{a_0} \quad 0 \quad \delta_{r_0} \quad 0]^T \\
x_{2_{\text{lat}}}(t) = [\delta_{a_b}(t) \quad \dot{\delta}_{a_b}(t) \quad \delta_{r_b}(t) \quad \dot{\delta}_{r_b}(t)]^T
\end{cases}
$$

Here, It assumed that longitudinal states is equipment states.

$$V_c = V_{c_0}, \alpha = \alpha_0, Q = Q_0, \Theta = \Theta_0 \tag{33}$$

When this time, linear system expressed are

$$\dot{\mathbf{x}}_{1_{\mathrm{lat}}} = A_{\mathrm{lat}} \mathbf{x}_{1_{\mathrm{lat}}} + B_{\mathrm{lat}} \mathbf{y}_{1_{\mathrm{latcom}}} \tag{34}$$

$$\mathbf{y}_{1_{\mathrm{lat}}} = C_{\mathrm{lat}} \mathbf{x}_{1_{\mathrm{lat}}}$$

$$P_{1_{\mathrm{lat}}}(s) = C_{\mathrm{lat}} \left(sE - A_{\mathrm{lat}}\right)^{-1} B_{\mathrm{lat}} \tag{35}$$

Where,

$$A_{\mathrm{lat}} = \begin{bmatrix} J_{1,33} & J_{1,34} & J_{1,36} & J_{37} \\ J_{1,43} - \sigma_{a,1_{\mathrm{lat}}} P_{\delta_a} - \sigma_{a,2_{\mathrm{lat}}} P_{\delta_r} & J_{1,44} - \sigma_{a,3_{\mathrm{lat}}} P_{\delta_a} - \sigma_{a,4_{\mathrm{lat}}} P_{\delta_r} & J_{1,46} - \sigma_{a,5_{\mathrm{lat}}} P_{\delta_a} - \sigma_{a,6_{\mathrm{lat}}} P_{\delta_r} & J_{47} - \sigma_{a,7_{\mathrm{lat}}} P_{\delta_a} - \sigma_{a,8_{\mathrm{lat}}} P_{\delta_r} \\ J_{1,63} - \sigma_{a,9_{\mathrm{lat}}} P_{\delta_a} - \sigma_{a,10_{\mathrm{lat}}} P_{\delta_r} & J_{1,64} - \sigma_{a,11_{\mathrm{lat}}} P_{\delta_a} - \sigma_{a,12_{\mathrm{lat}}} P_{\delta_r} & J_{1,66} - \sigma_{a,13_{\mathrm{lat}}} P_{\delta_a} - \sigma_{a,14_{\mathrm{lat}}} P_{\delta_r} & J_{1,67} - \sigma_{a,15_{\mathrm{lat}}} P_{\delta_a} - \sigma_{a,16_{\mathrm{lat}}} P_{\delta_r} \\ J_{73} & J_{74} & J_{76} & J_{77} \end{bmatrix}$$

$$B_{\mathrm{lat}} = \begin{bmatrix} 0 & 0 \\ \sigma_{b,1_{\mathrm{lat}}} P_{\delta_a} + \sigma_{b,2_{\mathrm{lat}}} P_{\delta_r} & \sigma_{b,3_{\mathrm{lat}}} P_{\delta_a} + \sigma_{b,4_{\mathrm{lat}}} P_{\delta_r} \\ \sigma_{b,5_{\mathrm{lat}}} P_{\delta_a} + \sigma_{b,6_{\mathrm{lat}}} P_{\delta_r} & \sigma_{b,7_{\mathrm{lat}}} P_{\delta_a} + \sigma_{b,8_{\mathrm{lat}}} P_{\delta_r} \\ 0 & 0 \end{bmatrix}, \quad C_{\mathrm{lon}} = \begin{bmatrix} 1 & 0 \\ 0 & 0 \\ 0 & 0 \\ 0 & 1 \end{bmatrix}^T$$

$\sigma_{a,i}$, $\sigma_{b,j}$ (i = 1, 2, …,16, j = 1, 2, …, 8) are complicated, the description will be omitted. And in this paper, these transfer functions(Eqs.(31), (35)) using hierarchy dynamic inversion called Short Period Linearized Transfer Function (SPLTF).

5. Stability analysis and numerical simulation

When it determines the control performance, designer have to utilize the pseudo-input as following Eq. (21). As condition of this analysis first hierarchy parameters determine as follows.

5.1. Stability analysis of LATF

For the linearized analysis, the natural frequencies of actuator are $\omega_{\delta a}, \omega_{\delta e}, \omega_{\delta r}$ = 0.6 – 6.0 [Hz] (each 0.3 [Hz]).

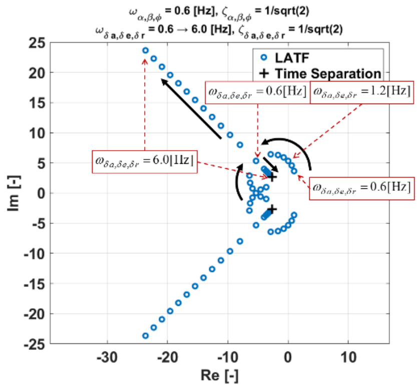

Fig. 3 Eigenvalue of LATF and designed.

As the characteristics of LATF, when damping coefficients are $\zeta_{\delta a,e,r} = 1/\sqrt{2}$, $\zeta_{\alpha,\beta,\phi} = 1/\sqrt{2}$. It shows that the ratio of the natural frequencies of aileron, elevator, and rudder actuators to designed frequencies of angle of attack, sideslip angle, and bank angle are required to be more twice times. And also, it shows that the ratio of the natural frequencies of aileron, elevator, and rudder actuators to designed frequencies of angle of attack, sideslip angle, and bank angle are required to be more four times in order to achieve the designed damping coefficient.

5.2. Numerical simulation

Actual control surfaces of the vehicle are elevons(has two functions of aileron and elevator), and rudder. Then, the transform from aileron, and elevator to each elevons are expressed as follows.

$$\begin{cases} \delta_{eL} = \delta_e - \delta_a \\ \delta_{eR} = \delta_e + \delta_a \end{cases} \tag{36}$$

Table 2 shows the initial condition, and Table 3 shows response characteristics patterns.

Table 2. Initial condition and target valuable.

Latitude	[-]	35°20’50.9”
Longitude	[-]	117°48’33.1”
Altitude	[m]	20000
Ground Speed	[m/s]	80
Angle of Attack	[deg.]	5
Side Slip Angle	[deg.]	0
Roll angle	[deg.]	0
Pitch angle	[deg.]	0
Yaw angle	[deg.]	180
Limit elevon angle	[deg.]	20
Limit rudder angle	[deg.]	20
Winged model	horizontal wind model	

Table 3. Each parameters.

Pattern		1	2	3
Natural frequencies $\omega_\alpha, \omega_\beta, \omega_\phi$	[Hz]	1.0	0.8	0.6
Actuator natural frequencies $\omega_{\delta_a}, \omega_{\delta_e}, \omega_{\delta_r}$	[Hz]	4	4	6
Frequency ratio ($\omega_{\alpha,\beta,\phi} / \omega_{\delta_a,\delta_e,\delta_r}$)	[-]	4	5	10
Damping coefficient $\zeta_\alpha, \zeta_\beta, \zeta_\phi$	[-]	$1/\sqrt{2}$	$1/\sqrt{2}$	$1/\sqrt{2}$
$\zeta_{\delta a,e,r}$	[-]	$1/\sqrt{2}$	$1/\sqrt{2}$	$1/\sqrt{2}$

Here, about commands (reference) of $\mathbf{y}_{1\mathrm{com}}$ are given from guidance law. Therefore, this numerical simulation does not evaluate the trajectory, and only evaluate attitude followability. Trajectory generator adopted the genetic algorithm proposed by miyamoto et al[21]. It assumed that the trajectory generator performs correction every 20 seconds from altitude 12 [km]. Fig. 4 shows the block diagram of the numerical simulation.

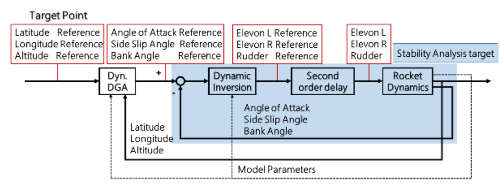

Fig. 4 Simulation Block Diagram.

Fig. 5-Fig. 11 show the simulation results of pattern 1 as a representative. Fig. 12-Fig. 17 are compare the eigenvalue each linearization method. These legend of without control mean the only vehicle eigenvalue(does not feedback control). Time Separation means the eigenvalue when it is ignore the second hierarchy dynamics(control designer can determine(Eq. (20))).

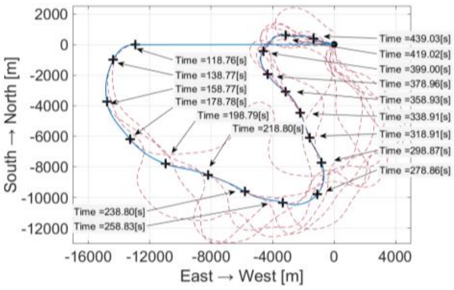

Fig. 5 Flight path result (pattern 1).

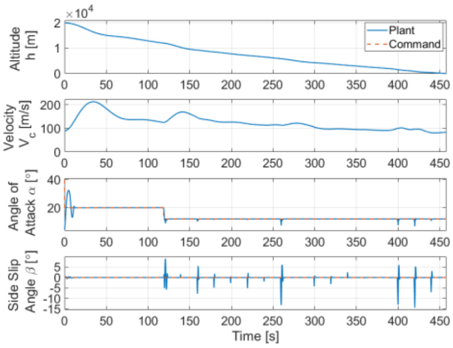

Fig. 6 Flight Profile-altitude, velocity, angle of attack side slip angle (pattern 1).

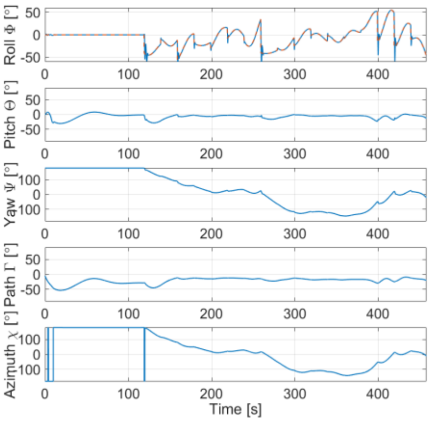

Fig. 7 Flight Profile-roll, pitch, yaw, path, azimuth angles (pattern 1).

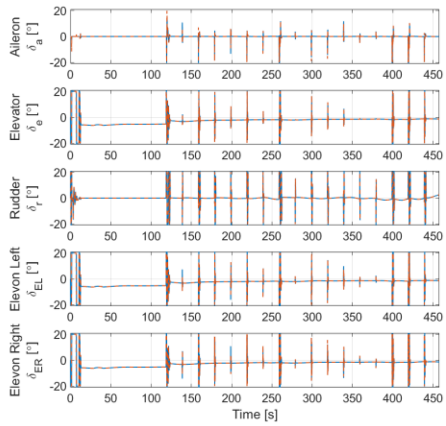

Fig. 8 Flight profile-aileron, elevator, rudder, elevon left, elevon right angles (pattern 1).

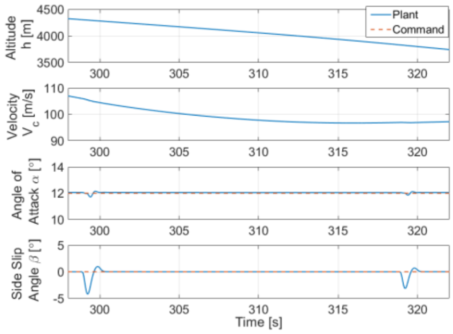

Fig. 9 Flight Profile-altitude, velocity, angle of attack side slip angle (298 – 322 [s]) (pattern 1).

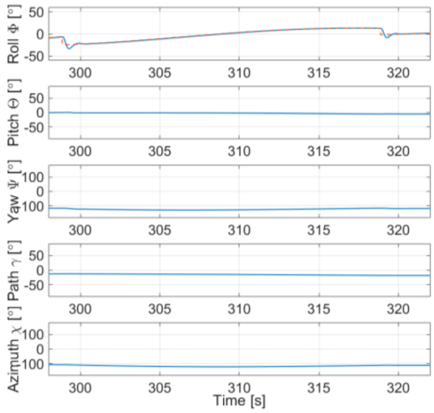

Fig. 10 Flight Profile-roll, pitch, yaw, path, azimuth angles (298 – 322 [s]) (pattern 1).

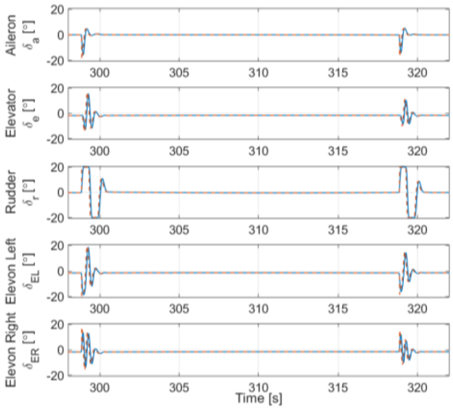

Fig. 11 Flight profile-aileron, elevator, rudder, elevon left, elevon right angles (298 – 322 [s]) (pattern 1).

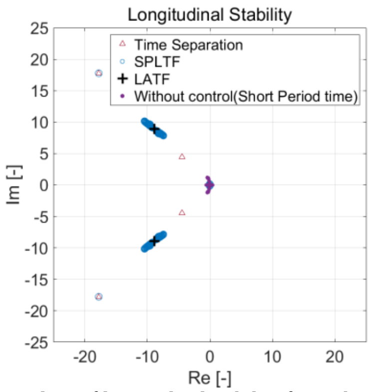

Fig. 12 Eigenvalues of longitudinal stability for each analysis method (pettern 1).

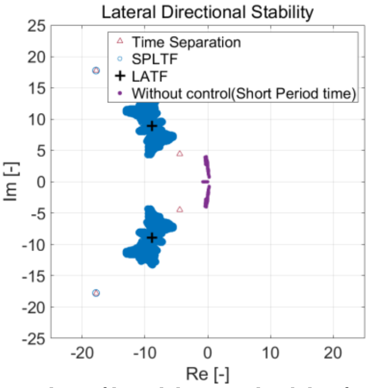

Fig. 13 Eigenvalues of lateral directional stability for each analysis method (pettern 1).

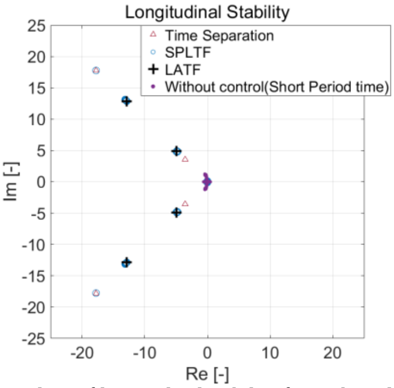

Fig. 14 Eigenvalues of longitudinal stability for each analysis method (pettern 2).

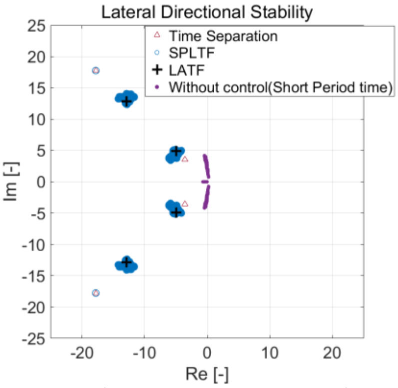

Fig. 15 Eigenvalues of lateral directional stability for each analysis method (pettern 2).

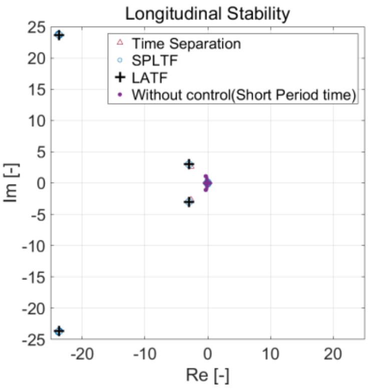

Fig. 16 Eigenvalues of longitudinal stability for each analysis method (pettern 3).

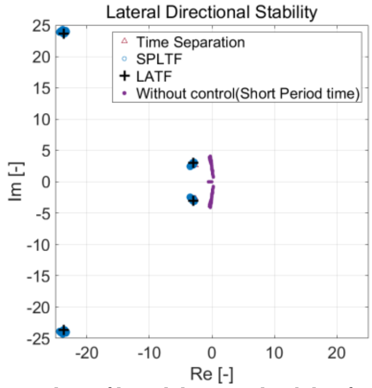

Fig. 17 Eigenvalues of lateral directional stability for each analysis method (pettern 3).

5.3 Discussions

In Fig. 5, trajectory generator renewal the quasi-optimal trajectory every 20 seconds, it is different the orbit every time. Then, It can be confirmed that control law using hierarchy DI follow flexibly various quasi-optimal trajectories. Fig. 6-Fig. 8 show the status during flight simulation, and Fig. 9-Fig. 11 is expanded during flight only from 298 to 322 seconds. it is rapid follow was observed according to the target states. It can be confirmed that stable all most of during flight from these results, but only the result of rudder angles reaches the saturation angles. Its cause the rudder performance is not so high, it is predicted that this is trying to move the control surface largely in order to satisfy the required performance response. However, this simulation is not divergence, it was not so much problem.
Fig. 12-Fig. 17 show the eigenvalue of longitudinal model, and lateral directional model each patterns. It was confirmed that enough stability was guaranteed enough. In addition, the major characteristics of eigenvalue analysis are as follows.

1. SPLTF exist not around time-separation, but around LATF.
2. LATF has the characteristic as the pole placement, and does not depend on the vehicle dynamics.
3. When the ratio of natural frequency is larger between first hierarchy and second hierarchy, the influence of nonlinear dynamics is smaller and smaller.
4. When the ratio of natural frequency is larger between first hierarchy and second hierarchy, the fluctuation range of SPLTF becomes smaller, and time separation becomes approaches LATF performance.

These characteristics also includes the time-scale separation, it possible to evaluate more globally than previous. In other words, the response of the actuator and the vehicle dynamics, it is possible to evaluate the influence, which could not confirmed by the time-scale separation by a relatively simple transfer function called LATF.

6. Conclusions

In this paper, the stability is evaluated in consideration of the dynamic characteristics of the second hierarchy. As a result, it found that clarified the existence of the nonlinear term which can not be completely canceled that by influence of the second hierarchy dynamics, and the linear term which is not depend on the characteristics of the vehicle dynamics. Then, it evaluated the influence of each terms on around the flight trajectory of the vehicle. In this model, the control performance using hierarchy dynamic inversion has been shown to have a affect of linear terms larger than that of nonlinear terms. In the numerical simulation, its control performance can be highly evaluated. Although it is difficult to evaluate to what influence of the nonlinear terms is small for general aircraft, it think that the influence is not so significant since the previous research as well. In the future, in order to realization utilize the hierarchy DI controller, it is necessary to evaluate the disturbance, parameter errors, authors are planning to study the influence each parameters, and evaluation method.

References

1) A. Ishidori,: Nonlinear Control System, *Springer-Verlab Berlin, Heidelberg*, (1995) , pp. 145-172
2) T. Gang,: Adaptive Control Design and Analysis, *John Wiley & Sons*, (2003) , pp. 535-541
3) M. Krstic, L. Kanellakopouios, and P. V. Kokotovic,: Nonlinear and Adaptive Control Design, *Wiley* (1995), pp. 64-66
4) P. K. A. Menon, et al.,: Nonlinear Flight Test Trajectory Controller for Aircraft, *Journal of Guidance, Control, and Dynamics*, **10(**1), (1987), pp. 67-72
5) P. K. A. Menon, et al.,: Nonlinear Missile Autopilot Design Using Time-Scale Separation, *Proceeding of the AIAA Guidance, Navigation, and Control Conference*, New Orleans, L.A., August, AIAA-97-3765, (1997), pp. 1791-1803
6) S. Sunasawa, H. Ohta, Nonlinear Flight Control for a Reentry Vehicle Using Inverse Dynamics Transformation, *Journal of the Japan Society for Aeronautical and Space Sciences (JSASS)*, **45**(516), (1997), pp. 52-61 (in Japanese)
7) Y. Baba, H. Takano, Flight Control Design Using Nonlinear Inverse Dynamics, *Journal of the Japan Society for Aeronautical and Space Sciences (JSASS)*, **47(**547), (1999), pp. 122-128 (in Japanese)
9) D. Ito, et al., Reentry Vehicle Flight Controls Design Guidelines: Dynamic Inversion, Technical Report, NASA/TP-2002-210771 (2002)
10) D. S. Naidu, and J. C. Anthony, Singular Perturbations and Time Scales in Guidance and Control of Aerospace Systems: A Survey, *Journal of Guicance, Control, and Dynamics*, **24(**6), (2001), pp. 1057-1078
11) P. Kokotovic, et al, Singular Perturbation methods in control analysis and design, *Society for Industrial and Applied Mathematics*, (1999), pp. 17-40
12) J. Kawaguchi, Y. Miyazawa, T. Ninomiya, Flight Control Law Design with Hierarchy-Structured Dynamic Inversion Approach, *Proceeding of the AIAA Guidance, Navigation, and Control Conference*, Honolulu, Hawaii, August, (2008), AIAA-2008-6959
13) J. Kawaguchi, T. Ninomiya, H. Suzuki, GUIDANCE AND CONTROL FOR D-SEND#2, *International Congrees of the Aeronautical Sciences(ICAS)*, Brisbane, Australia, September, (2012), 2012-5.3.1
14) T. Ninomiya, H. Suzuki, J. Kawaguchi, Evaluation of Guidance and Control System of D-SEND#2, *IFAC-PapersOnline*, **49(**17), (2016), pp. 106-111
15) T. Ninomiya, H. Suzuki, J. Kawaguchi, Controller Design for D-SEND#2, *Journal of the Japan Society for Aeronautical and Space Sciences (JSASS)*, **64**(3), (2016), pp. 160-170 (in Japanese)
16) A. Abe, Y. Shimada, Flight Control System Using Backstepping Method for Space Transportation System, *Transactions of the Society for Aeronautical and Space Sciences, Aerospace Technology Japan*, **10**-ists28, (2012), Pd_85/Pd_91
17) A. Abe, K. Iwamoto, Y. Shimata, Design of Flight Control System Based on Adaptive Backstepping Method for a Space Transportation System, *Transactions of the Japan Society for Aeronautical and Space Sciences*, **58**(2), (2015), pp. 55-65
16) G. Guna Surendra, et al, Recent Developments of Experimental Winged Rocket: Autonomous Guidance and Control Demonstration Using Parafoil, *Procedia Engineering*, **99**, (2015), pp. 156-162
17) K. Itakura, et al., Development and Ground Combustion Test of a Subscale Reusable Winged Rocket, *Transactions of the Society for Aeronautical and Space Sciences, Aerospace Technology Japan*, **12**-ists29, (2014), To_3_1/To_3_5
18) T.Ohki, et al., Recent Developments of Experimental Winged Rocket: Autonomous Guidance and Control Demonstration by Flight Test, *Asia-Pacific International Symposium on Aerospace Tchnology*, Cairns, Australia, (2015), pp. 408-414
19) K. Yonemoto, T. Fujikawa, et al, Recent Flight Test of Experimental Winged Rocket and Its Future Plan for Suborbital Technology Demonstration, *International Astronautical Congress (IAC)*, Guadalajara, Mexico, September, (2016), pp. IAC-16-D2.6.1
20) H. Yamasaki, K. Yonemoto, et al., Linearization and Response Analysis of Flight Dynamics Equations Using Multi-Hierarchy Dynamic Inversion, *Japan Joint Automatic Control Conference* 59th, Kitakyushu, Japan, (2016), pp.1054-1059 (in Japanese)
21) S. Miyamoto, T. Narumi, T. Matsumoto, Y. Yonemoto, Real-time Guidance of Reusable Winged Space Plane Using Genetic Algorithm Implemented on Field Programmable Gate Array, *Advanced Intelligent Mechatrocics (AIM)*, KaoHsiung, Taiwan, (2012), pp. 349-354